

# Jet Charge: A Flavor Prism for Spin Asymmetries at the EIC

Zhong-Bo Kang,<sup>1,2,3,\*</sup> Xiaohui Liu,<sup>4,5,†</sup> Sonny Mantry,<sup>6,‡</sup> and Ding Yu Shao<sup>1,2,3,§</sup>

<sup>1</sup>*Department of Physics and Astronomy, University of California, Los Angeles, California 90095, USA*

<sup>2</sup>*Mani L. Bhaumik Institute for Theoretical Physics,*

*University of California, Los Angeles, California 90095, USA*

<sup>3</sup>*Center for Frontiers in Nuclear Science, Stony Brook University, Stony Brook, New York 11794, USA*

<sup>4</sup>*Center of Advanced Quantum Studies, Department of Physics,  
Beijing Normal University, Beijing 100875, China*

<sup>5</sup>*Center for High Energy Physics, Peking University, Beijing 100871, China*

<sup>6</sup>*Department of Physics and Astronomy, University of North Georgia, Dahlonega, GA 30597, USA*

We propose the jet charge observable as a novel probe of flavor structure in the nucleon spin program at the Electron Ion Collider (EIC). We show that jet charge measurements can substantially enhance the sensitivity of spin asymmetries to different partonic flavors in the nucleon. This sensitivity can be further improved by constructing the jet charge using only a subset of hadron species (pions or kaons) in the jet. As an example, we use the Sivers asymmetry in back-to-back electron-jet production at the EIC to show that the jet charge can be a unique tool in constraining the Sivers function for different partonic flavors.

*Introduction.* The femtoscale structure of the nucleon is a central mission of current experimental programs at accelerator facilities such as the Relativistic Heavy Ion Collider (RHIC) at Brookhaven National Lab, 12 GeV CEBAF at Jefferson Lab, COMPASS at CERN, and HERMES at DESY. It is also one of the major scientific pillars of the future Electron Ion Collider (EIC) [1, 2]. In particular, the flavor and spin structure of the nucleon in terms of both one dimensional (1D) and three-dimensional (3D) imaging provides fascinating glimpses into the highly nontrivial non-perturbative QCD dynamics.

One of the major available tools to effectively deconvolute the experimental information on the flavor and spin structure of the nucleon as encoded in unpolarized and polarized parton distribution functions (PDFs) and their extensions such as transverse momentum distributions (TMDs), is the “global QCD analysis”. It treats all available probes/processes simultaneously to extract the set of universal PDFs. For example, for the polarized PDFs, one relies on polarized inclusive deep inelastic scattering (DIS), semi-inclusive DIS (SIDIS), and proton-proton collisions [3]. In general, fully inclusive DIS data is difficult to disentangle different quark flavors, unless one uses different targets such as the proton, deuteron, and <sup>3</sup>He [4, 5]. In this regard, the SIDIS process is crucial: it uses the detection of charged pions or kaons in the final state as a flavor tag of the initial-state PDFs, provided the fragmentation functions are well known [6].

In recent years, measurements at RHIC and LHC demonstrate that jets can be a useful probe for the spin structure of the nucleon [7–9]. The advent of the EIC with its high luminosity and polarized beams will unlock the full potential of jets as novel tools for probing nucleon structure. It is thus not a surprise that jet physics at the EIC has become a fast emerging field of research [10–18]. While a lot of progress has been made in jet physics at the

EIC, flavor separation in jet production and the associated spin asymmetries presents a major challenge and has not been addressed in the literature. As collimated spray of hadrons, jet observables are typically inclusive over the final-state hadrons within the jet. As a consequence, although jets are better proxies of parton-level dynamics, they typically lack flavor tagging, as used extensively in traditional SIDIS observables. However, it is well-known that flavor separation is essential in mapping out the flavor and spin structure of the nucleon at the EIC. Within this context, there has now been some recent work on jet fragmentation functions, see Refs. [16, 19], where measuring the distribution of hadrons inside jets allows for some amount of flavor separation.

In this paper, we propose utilizing the jet charge observable [20] as a novel flavor prism for jet observables at the EIC, especially for spin asymmetries in jet production. Jet charge has been studied extensively at the LHC [21–25], and similar directions at the RHIC are being currently explored [26, 27]. We develop a theoretical framework which allows us to distinguish flavor in spin asymmetries, enabling jet production processes to reach their full potential in probing the flavor and spin structure of the nucleon. As a concrete example, we demonstrate for the first time the use of the jet charge observable to provide enhanced *u*- and *d*-quark flavor sensitivity for both the unpolarized quark TMDs and the polarized Sivers TMD functions using back-to-back electron-jet production at the EIC. The unpolarized TMDs are essential for the 3D imaging of the nucleon in momentum space and the Sivers TMD functions, in addition, encode quantum correlations between the motion of partons and the spin of the proton.

*Jet charge.* The standard jet electric charge is constructed from the definition [28, 29]

$$Q_{\kappa}^i = \sum_h Q_{\kappa}^h \equiv \sum_{h \in \text{jet}} z_h^{\kappa} Q_h, \quad (1)$$

where a parton of species  $i$  initiates the jet and  $\kappa$  is a parameter that is part of the definition. The fraction of the jet transverse momentum carried by hadron  $h$  with electric charge  $Q_h$  (in units of the positron charge  $e$ ) is denoted by  $z_h = p_T^h/p_T$ , where  $p_T^h$  and  $p_T$  denote the transverse momenta of the hadron and the jet, respectively. Note that the definition of  $Q_\kappa^i$  allows for the option of defining the jet charge by restricting the sum over hadrons  $h$  in the jet to include only particular species. For instance, one could restrict the sum to include only the charged pions or kaons. This flexibility can be exploited for additional flavor separation.

*Unpolarized TMDs.* We first consider the unpolarized electron-proton scattering process,  $e+p \rightarrow e+\text{jet}+X$ . In order to access TMD dynamics, we consider the back-to-back region where the electron-jet transverse momentum imbalance is small. The contribution to the cross section from the  $i$ -th parton in the proton is given by the factorization formula [10–12]

$$\frac{d\sigma_{UU}^i}{dy_e d^2p_T^e d^2q_T} = \sigma_0 e_i^2 \int \frac{d^2b_T}{(2\pi)^2} e^{iq_T \cdot b_T} \tilde{W}_i, \quad (2)$$

where  $y_e$  and  $\vec{p}_T^e$  denote the lepton rapidity and transverse momentum, respectively, and  $q_T$  is the jet-lepton transverse momentum imbalance with  $|\vec{q}_T| = |\vec{p}_T^e + \vec{p}_T| \ll p_T^e \sim p_T$  of the jet. The spin-averaged structure function  $\tilde{W}_i$  for parton  $i$  has the factorized form

$$\tilde{W}_i = \tilde{f}_i(x, b_T, \mu) S_J(b_T, R, \mu) H(Q, \mu) \mathcal{J}_i(p_T R, \mu), \quad (3)$$

where  $Q^2$  is the invariant mass of the virtual photon, and detailed definitions of the various objects appearing above can be found in [10–12].  $\mathcal{J}_i(p_T R, \mu)$  is the universal jet function that describes the dynamics of the jet initiated by the struck parton of flavor  $i$  [30–32].  $\tilde{f}_i(x, b_T, \mu)$  is the Fourier transform of the unpolarized TMD function  $f_i(x, k_T, \mu)$ , that gives the distribution in the longitudinal momentum fraction  $x$  and the transverse momentum  $k_T$  of the parton  $i$  in the proton [33].

The measured cross section includes a sum over all partonic channels so that  $d\sigma_{UU} = \sum_i d\sigma_{UU}^i$ . Thus, it is sensitive only to a specific flavor combination of TMDs. However, by making an additional measurement of the jet charge and grouping the data into jet charge bins, one can enhance or suppress sensitivity to TMDs of different flavors. The generalization of Eq. (2) in which the jet charge is also measured is achieved by replacing  $\mathcal{J}_i(p_T R, \mu)$  with the function  $\mathcal{G}_i(Q_\kappa^i, p_T R, \mu)$  [29] which also includes the probability that the jet charge has the value  $Q_\kappa^i$ . It is normalized as

$$\int dQ_\kappa^i \mathcal{G}_i(Q_\kappa^i, p_T R, \mu) = \mathcal{J}_i(p_T R, \mu), \quad (4)$$

so that integrating over all possible jet charge values gives back the standard jet function.

Since the generalization of Eq. (2) to include a jet charge measurement is achieved simply by the replacement  $\mathcal{J}_i \rightarrow \mathcal{G}_i$ , the renormalization scale independence of the cross section implies that the renormalization group evolution properties of  $\mathcal{G}_i$  are exactly the same as  $\mathcal{J}_i$  [11, 34].

The universality of the jet function  $\mathcal{J}_i$  implies that it appears in the factorization formulae of different processes such as exclusive Boson+1-jet production [34–38] and threshold single inclusive jet production [39] in  $pp$  collisions, and jet production in  $e^+e^-$  collisions [32]. This universality also applies to the  $\mathcal{G}_i$  function with these observables modified to include a jet charge measurement. Since the jet charge in Eq. (1) is defined at the hadron level, the jet charge distribution function  $\mathcal{G}_i$  is sensitive to the hadronization, giving rise to nonperturbative effects that can be constrained through its universality.

For the analysis of the jet charge binned data it becomes useful to characterize each jet charge bin by the value of its jet charge moment. The  $N$ -th moment of the jet charge in a particular jet charge bin is given by

$$\langle (Q_\kappa^i)^N \rangle_{\text{bin}} = \int_{Q_\kappa^i\text{-bin}} dQ_J Q_J^N \frac{\mathcal{G}_i(Q_J, p_T R, \mu)}{\mathcal{J}_i(p_T R, \mu)}. \quad (5)$$

If we restrict the jet charge to lie in a particular jet charge bin, with the  $N$ -th moment of the jet charge  $\langle (Q_\kappa^i)^N \rangle_{\text{bin}}$  for jets initiated by parton  $i$ , the corresponding factorization formula for the total cross section is given by

$$\frac{d\sigma_{UU}(Q_{\kappa, \text{bin}}^N)}{dy_e d^2p_T^e d^2q_T} = \sum_{i=u, d, \dots} \langle (Q_\kappa^i)^N \rangle_{\text{bin}} \frac{d\sigma_{UU}^i}{dy_e d^2p_T^e d^2q_T}, \quad (6)$$

which immediately follows from a comparison of Eqs. (2–5). This is a key result that allows for flavor separation of the TMDs through an appropriate selection of jet charge bins that can enhance or suppress the contribution of the  $i$ -th parton flavor depending on the value of  $\langle (Q_\kappa^i)^N \rangle_{\text{bin}}$ , relative to that of other parton flavors.

Note that the universality of  $\mathcal{G}_i$  and  $\mathcal{J}_i$  make the moments  $\langle (Q_\kappa^i)^N \rangle_{\text{bin}}$  process independent, allowing for their extraction from a global analysis that makes use of binned jet charge measurements in the electron-proton scattering,  $pp$  collisions, and  $e^+e^-$  annihilation processes with appropriate kinematic cuts. Furthermore, the binned jet charge moments  $\langle (Q_\kappa^i)^N \rangle_{\text{bin}}$  are  $\mu$ -independent due to a cancellation of the scale dependence between  $\mathcal{J}_i$  and  $\mathcal{G}_i$  in Eq. (5).

The jet charge moments do however have a mild dependence on  $p_T R$  via loop suppressed effects [29]. This loop suppression can be understood by noting that at tree-level the jet consists of single parton evolving into hadrons. The  $p_T R$  dependence first arises at the next-to-leading order through a perturbative splitting within the jet before hadronization. We have checked this behavior via Pythia8 [40] simulations over a wide range of

$p_T R$  for  $\kappa = 0.3$ . This property can allow for the extraction of the jet charge moments from jet observables over a wide range of kinematics.

In addition, as expected from Eqs. (4) and (5), the zeroth and first moments have to satisfy the sum rules

$$\sum_{\text{bins}} \langle (Q_\kappa^i)^0 \rangle_{\text{bin}} = 1, \quad \sum_{\text{bins}} \langle Q_\kappa^i \rangle_{\text{bin}} = \langle Q_\kappa^i \rangle, \quad (7)$$

corresponding to the fact that the sum over all jet charge bin fractions is unity and the sum over all binned average jet charges is the average jet charge over all bins. These sum rules provide additional constraints that can be used in a global analysis of the binned jet charge moments. The average jet charge over all bins can be related [28, 29] to the hadron fragmentation functions as  $\langle Q_\kappa^i \rangle = \sum_h Q_h \mathcal{J}_{ij}(\kappa) D_j^h(\kappa)$ , where  $D_j^h(\kappa)$  and  $\mathcal{J}_{ij}(\kappa)$  are the  $\kappa$ -th moments of the  $j \rightarrow h$  fragmentation function  $D_j^h(z)$  and the perturbatively calculable matching coefficient that describes the  $i \rightarrow j$  parton splitting inside the jet, respectively. At lowest order, the matching coefficient takes the form  $\mathcal{J}_{ij}(\kappa) = \delta_{ij} + \mathcal{O}(\alpha_s(p_{J,T}R))$ .

The jet charge moments of different species will also be related by QCD flavor and charge conjugation symmetries, further reducing the number of fit parameters. Furthermore, as seen in Eq. (6), the jet charge moments  $\langle (Q_\kappa^i)^N \rangle_{\text{bin}}$  only affect the relative size of each partonic contribution and not the shapes of their kinematic distributions.

All of these features facilitate the extraction of the jet charge moments through a global analysis. In fact, measurements of the jet charge distribution has already been carried out in both  $pp$  and  $PbPb$  collisions at the LHC [21, 22, 25].

*Single Spin Asymmetry.* One can generalize the factorization to the process  $e + p(S_\perp) \rightarrow e + \text{jet} + X$  where the proton is transversely polarized with spin vector  $\vec{S}_\perp$ . In this case, the cross section takes the form  $d\sigma(S_\perp) = d\sigma_{UU} + d\sigma_{UT}(S_\perp)$ , where the additional spin-dependent contribution  $d\sigma_{UT}$  depends on the Siverson function [41]. The cross section for the partonic channel  $i$  is given by [10–12]

$$\frac{d\sigma_{UT}^i(S_\perp)}{dy_e d^2p_T^e d^2q_T} = e_i^2 \sigma_0 \epsilon_{\alpha\beta} S_\perp^\alpha \int \frac{d^2b_T}{(2\pi)^2} e^{iq_T \cdot b_T} \tilde{W}_{T,i}^\beta, \quad (8)$$

where the spin-dependent structure function  $\tilde{W}_{T,i}$  takes the factorized form

$$\tilde{W}_{T,i}^\beta = \tilde{f}_{1T,i}^{\perp,\beta}(x, b_T, \mu) S_J(b_T, R, \mu) H(Q, \mu) \mathcal{J}_i(p_T R, \mu),$$

where  $\tilde{f}_{1T,i}^{\perp,\beta}(x, b_T, \mu)$  is the Fourier transform of the Siverson function [10–12]. The Siverson function can be directly accessed via the single spin asymmetry

$$A_{UT} = \frac{d\sigma(S_\perp^\uparrow) - d\sigma(S_\perp^\downarrow)}{d\sigma(S_\perp^\uparrow) + d\sigma(S_\perp^\downarrow)} = \frac{d\Delta\sigma_{UT}}{d\sigma_{UU}}, \quad (9)$$

where  $d\Delta\sigma_{UT} = [d\sigma_{UT}(S_\perp^\uparrow) - d\sigma_{UT}(S_\perp^\downarrow)]/2$ . Following the same steps used to arrive at Eq. (6) for the unpolarized case, the single spin asymmetry in a particular jet charge bin,  $A_{UT}^{\text{bin}}$ , is given by

$$A_{UT}^{\text{bin}} = \sum_{i=u,d,\dots} \langle (Q_\kappa^i)^N \rangle_{\text{bin}} A_{UT}^i, \quad (10)$$

where  $A_{UT}^i = d\Delta\sigma_{UT}^i/d\sigma_{UU}$  is the contribution of the parton of flavor  $i$  to  $A_{UT}$ . Similar to Eq. (6), this is another key result that allows for flavor separation of the Siverson function. Note that the moments  $\langle (Q_\kappa^i)^N \rangle_{\text{bin}}$  that appear here are the same as the ones in Eq. (6).

The dominant contribution to  $A_{UT}$  is known to come from the  $u$ -quark channel [11, 42] because of the enhancement from the charge  $e_u^2$ , resulting in sensitivity primarily to the  $u$ -quark Siverson function. However, using Eq. (10),  $A_{UT}^{\text{bin}}$  can be used to enhance sensitivity to the Siverson functions of the other quark flavors through an appropriate selection of jet charge bins.

*Phenomenology.* We present numerical results to demonstrate the implications of the key results in Eqs. (6) and (10). We work in electron-proton center-of-mass (CM) frame with CM energy  $\sqrt{s} = 105$  GeV. We apply event selection cuts of  $Q^2 \geq 10$  GeV<sup>2</sup>,  $0.1 \leq y \leq 0.9$ , and  $15$  GeV  $\leq p_T^e \leq 20$  GeV,  $q_T \leq 2.5$  GeV, and  $10$  GeV  $\leq p_T \leq 25$  GeV, where  $y$  denotes the inelasticity. Jets are constructed using anti- $k_T$  jet algorithm [43] with radius parameter  $R = 1$ . For the back-to-back electron-jet production, the gluon TMD does not contribute so that the quark TMDs can be probed cleanly.

We first present results for the unpolarized case. For calibration purposes, we check the consistency between Pythia8 simulations and the theoretical predictions. The

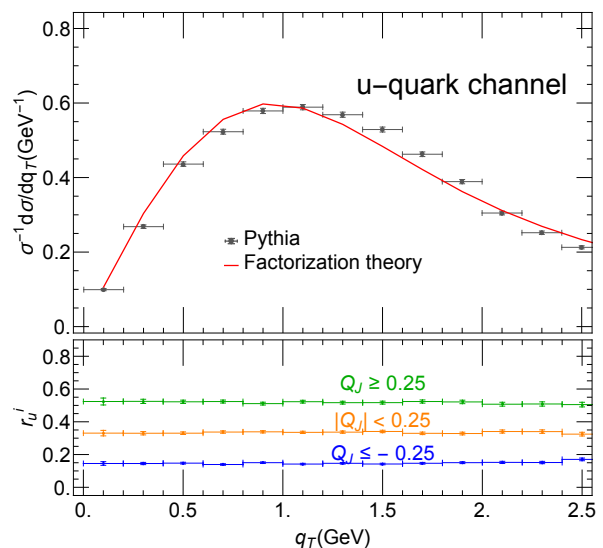


FIG. 1: The contribution of the  $u$ -quark TMD to the  $q_T$ -distribution.

	$u$	$\bar{u}$	$d$	$\bar{d}$	$s$	$\bar{s}$
$r_i^+$	0.52	0.17	0.15	0.53	0.30	0.34
$r_i^-$	0.15	0.49	0.52	0.15	0.36	0.32
$r_i^0$	0.33	0.35	0.33	0.32	0.35	0.34

TABLE I: The jet charge bin fractions  $r_i^{\pm,0}$  for various quark flavors, obtained from Pythia8 simulations.

upper panel in Fig. 1 shows a comparison of the  $q_T$ -distribution between Pythia simulations and the prediction of Eq. (2), where only the  $u$ -quark contribution is included.

Eq. (2) is evaluated at the next-to-leading logarithmic level of accuracy, with all functions in the factorization formula evaluated at  $\mathcal{O}(\alpha_s)$ , and with non-global logarithms included [10–12, 38, 44]. We parameterize the  $u$ -quark TMD function following Ref. [11]. In Fig. 1, we see good agreement between the simulation and theory for the normalized  $q_T$ -distribution.

Next we turn to  $q_T$ -distribution in different jet charge bins. The jet charges are constructed using Eq. (1) with  $\kappa = 0.3$  and only including charged pions in the sum over hadrons. Thus, if a jet contains no charged pions its charge vanishes. We denote the jet charge by  $Q_J$  and divide the data into three jet charge bins. The negative (“−”) bin with  $Q_J \leq -0.25$ , the neutral bin (“0”) with  $|Q_J| < 0.25$ , and the positive bin (“+”) with  $Q_J \geq 0.25$ .

The lower panel of Fig. 1 shows the jet charge bin fractions  $r_u^{\pm,0} \equiv \langle (Q_u^{\pm,0})_{\pm,0} \rangle$  for the  $u$ -quark jets as a function of  $q_T$ . These bin fractions were determined from Pythia simulations and are found to be independent of  $q_T$ . This agrees with the universality as expected from our factorization theorem. In Tab. I, we summarize the  $r_i^{\pm,0}$  values, including other quark flavors. We find that  $r_u \approx r_{\bar{d}}$ ,  $r_d \approx r_{\bar{u}}$  and  $r_s \approx 1 - r_{\bar{s}}$  as expected from the QCD flavor and charge conjugation symmetries and the fact that only charged pions were included in constructing the jet charge. A jet charge based only on charged kaons can increase the negative charge bin fractions of the  $s$ -quarks by a factor of  $\mathcal{O}(5)$  with respect to the  $u(d)$ -quark fraction, allowing for better sensitivity to the strange quark TMD and Sivvers functions.

The values in Tab. I are used as inputs in the rest of the analysis to make theoretical predictions for the relative size of contributions from different quark flavors to the  $q_T$ -distribution in each jet charge bin. In practice, the bin fractions  $r_i^{\pm,0}$  for each parton flavor could be obtained with a fit of the the cross section in Eq. (6) to the  $q_T$  spectrum in each charge bin, and used as inputs for theoretical predictions of the  $A_{UT}^{\text{bin}}$  in Eq. (10).

From the first and third columns in Tab. I, in the negative bin the size of the  $u$ -quark contribution will be significantly reduced and the relative  $d$ -quark contribution will be enhanced, compared to the neutral and positive

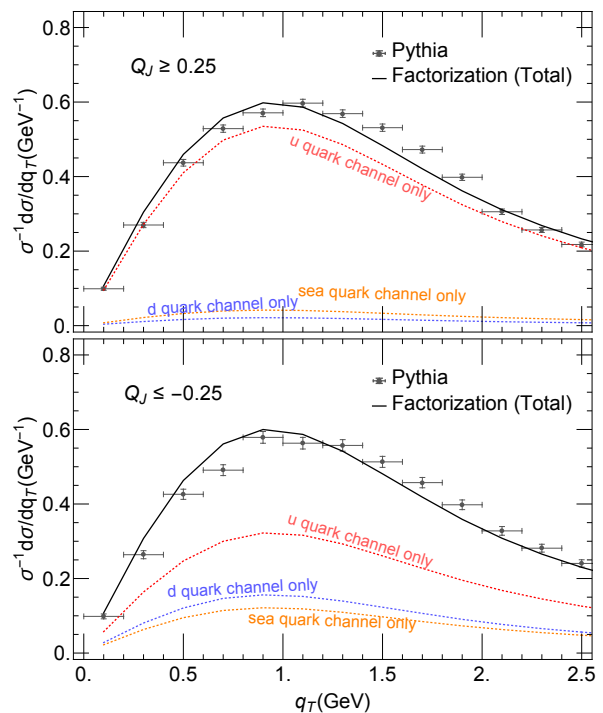


FIG. 2: The relative size of contributions from the unpolarized  $u$ -,  $d$ -, and sea quark TMDs to the  $q_T$ -distribution, in  $Q_J \geq 0.25$  (top) and  $Q_J \leq -0.25$  (bottom) charge bins.

bins. This can be seen in Fig. 2, where for  $Q_J \geq 0.25$  (upper panel), the  $d$ -quark and the sea quark contributions are highly suppressed and the  $u$ -quark contribution dominates the bulk of the distribution. On the other hand, for  $Q_J \leq -0.25$  (bottom panel) the  $u$ -quark contribution is now suppressed and the  $d$ - and sea quark contributions are relatively enhanced and more readily accessible in experiment.

Next we investigate the single spin asymmetry. Fig. 3 shows a comparison of the theoretical predictions for the standard asymmetry  $A_{UT}$  with the binned asymmetries

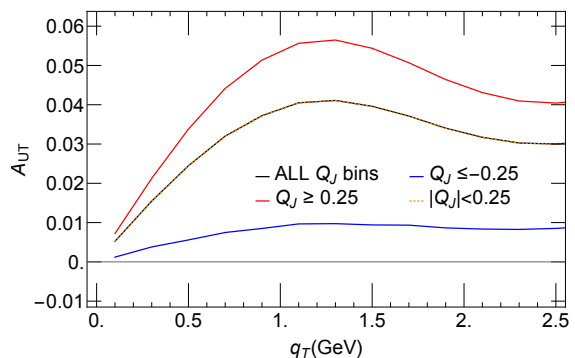


FIG. 3: Theoretical predictions for the Sivvers asymmetry in different jet charge bins.

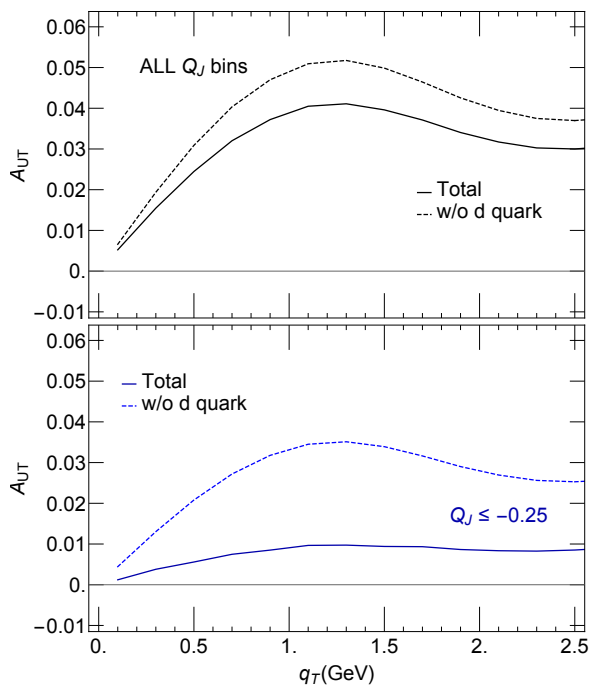


FIG. 4: Sensitivities of the  $u$ - and  $d$ -quark channels to the standard Sivvers asymmetry (top) and the Sivvers asymmetry in the  $Q_J \leq -0.25$  bin (bottom).

$A_{UT}^{\text{bin}}$  given in Eq. (10). The predictions can be compared with the future measurements. For the theoretical predictions of  $A_{UT}^{\text{bin}}$  in Fig. 3, bin fractions from Tab. I are used and the Sivvers functions are parameterized following Ref. [45], except that we ignore the strange quark Sivvers functions in light of recent global analysis which shows the very small size of their contributions [46]. Nevertheless, we note once again, for a jet charge based only the charged kaons in the jet, an appropriate choice of the jet charge bin can make  $A_{UT}^{\text{bin}}$  sensitive to the  $s(\bar{s})$ -Sivvers functions.

From Fig. 3, we see that  $A_{UT}$  is positive and large for  $Q_J \geq 0.25$  which is due to the dominant  $u$ -quark Sivvers function which gives a positive contribution, while the other channels are highly suppressed. On the other hand, in the  $Q_J \leq -0.25$  bin, the  $u$ -quark contribution is substantially reduced and comparable to the size of the  $d$ -quark contribution. Thus, the cancellation between the  $u$ - and  $d$ -quark Sivvers functions leads to a small spin asymmetry for  $Q_J \leq -0.25$ . For the  $|Q_J| < 0.25$  bin, since the bin fractions are roughly the same for all partonic channels, as seen in Tab. I, the spin asymmetry is expected to be close to the standard  $A_{UT}$ , as seen in Fig. 3. Similar behavior is observed for the single spin asymmetry in SIDIS when charged pions are measured [47]. In other words, the Sivvers asymmetry by selecting jet charge bins ( $Q_J > 0.25$  vs  $Q_J < -0.25$ ) plays a similar role as the SIDIS process by detecting pions in the final state ( $\pi^+$  vs  $\pi^-$ ).

Finally, we study the sensitivity of  $A_{UT}$  and  $A_{UT}^{\text{bin}}$  to different quark flavors. As seen in the top panel of Fig. 4, the standard Sivvers asymmetry is not sensitive to the  $d$ -quark Sivvers function, since the size of the asymmetry  $A_{UT}$  changes only slightly when one removes the  $d$ -quark contribution (“w/o  $d$ -quark”). However, if one restricts to the  $Q_J \leq -0.25$  bin, removing the  $d$ -quark contribution leads to a significant change in the asymmetry  $A_{UT}$  as seen in the bottom panel of Fig. 4. This demonstrates the dramatically enhanced sensitivity to the valence  $d$ -quark contribution in  $A_{UT}^{\text{bin}}$ . Thus, a measurement of the single spin asymmetry in the  $Q_J \leq -0.25$  bin can improve constraints on the  $d$ -quark Sivvers function.

*Conclusions.* In this work, we propose the jet charge as a unique flavor probe of polarized and unpolarized TMDs at the EIC. As a concrete example, we study back-to-back electron-jet production and we give predictions for the small transverse momentum imbalance  $q_T$ -distribution and the Sivvers asymmetry in different jet charge bins, based on a factorization framework. In order to demonstrate its power for flavor separation, we compare the flavor sensitivities of the jet charge binned unpolarized cross section and the Sivvers spin asymmetries with their standard counterparts at the EIC. We show that the jet charge can be used to enhance the sensitivity to the unpolarized TMDs and Sivvers functions of different quark species through an appropriate selection of the charge bins. Furthermore, the flavor sensitivity can be improved even more when specific subset of hadron species are used to define the jet charge. We expect the ideas proposed in this work to open new directions of exploration for jet/spin physics at the future EIC.

*Acknowledgements.* We thank Nobuo Sato for valuable discussions. This work is supported by the National Science Foundation under Contract No. PHY-1720486 and CAREER award PHY-1945471 (Z.K., D.Y.S.), by the National Natural Science Foundation of China under Grant No. 11775023 (X.L.), and by Center for Frontiers in Nuclear Science of Stony Brook University and Brookhaven National Laboratory (D.Y.S.).

\* zhang@physics.ucla.edu

† xiliu@bnu.edu.cn

‡ mantry147@gmail.com

§ dingyu.shao@physics.ucla.edu

- [1] A. Accardi *et al.*, Eur. Phys. J. A **52**, 268 (2016), arXiv:1212.1701.
- [2] C. A. Aidala *et al.*, *Probing Nucleons and Nuclei in High Energy Collisions* (WSP, 2020), arXiv:2002.12333.
- [3] D. De Florian, G. A. Lucero, R. Sassot, M. Stratmann, and W. Vogelsang, Phys. Rev. D **100**, 114027 (2019), arXiv:1902.10548.
- [4] R. Milner, (2018), arXiv:1809.05626.
- [5] J. Maxwell and R. Milner, (2019), arXiv:1911.06650.
- [6] JAM, N. Sato, C. Andres, J. Ethier, and W. Melnitchouk,

- Phys. Rev. D **101**, 074020 (2020), arXiv:1905.03788.
- [7] E.-C. Aschenauer *et al.*, (2016), arXiv:1602.03922.
- [8] STAR, L. Adamczyk *et al.*, Phys. Rev. D **97**, 032004 (2018), arXiv:1708.07080.
- [9] D. Boer and C. Pisano, Phys. Rev. D **91**, 074024 (2015), arXiv:1412.5556.
- [10] X. Liu, F. Ringer, W. Vogelsang, and F. Yuan, Phys. Rev. Lett. **122**, 192003 (2019), arXiv:1812.08077.
- [11] M. Arratia, Z.-B. Kang, A. Prokudin, and F. Ringer, (2020), arXiv:2007.07281.
- [12] X. Liu, F. Ringer, W. Vogelsang, and F. Yuan, (2020), arXiv:2007.12866.
- [13] E.-C. Aschenauer, K. Lee, B. Page, and F. Ringer, Phys. Rev. D **101**, 054028 (2020), arXiv:1910.11460.
- [14] M. Arratia, Y. Song, F. Ringer, and B. Jacak, Phys. Rev. C **101**, 065204 (2020), arXiv:1912.05931.
- [15] M. Arratia, Y. Makris, D. Neill, F. Ringer, and N. Sato, (2020), arXiv:2006.10751.
- [16] Z.-B. Kang, K. Lee, and F. Zhao, (2020), arXiv:2005.02398.
- [17] E. Aschenauer *et al.*, Rept. Prog. Phys. **82**, 024301 (2019), arXiv:1708.01527.
- [18] L. Zheng, E. Aschenauer, J. Lee, B.-W. Xiao, and Z.-B. Yin, Phys. Rev. D **98**, 034011 (2018), arXiv:1805.05290.
- [19] Z.-B. Kang, A. Prokudin, F. Ringer, and F. Yuan, Phys. Lett. B **774**, 635 (2017), arXiv:1707.00913.
- [20] R. Field and R. Feynman, Nucl. Phys. B **136**, 1 (1978).
- [21] ATLAS, G. Aad *et al.*, Phys. Rev. D **93**, 052003 (2016), arXiv:1509.05190.
- [22] CMS, A. M. Sirunyan *et al.*, JHEP **10**, 131 (2017), arXiv:1706.05868.
- [23] H. T. Li and I. Vitev, Phys. Rev. D **101**, 076020 (2020), arXiv:1908.06979.
- [24] S.-Y. Chen, B.-W. Zhang, and E.-K. Wang, Chin. Phys. C **44**, 024103 (2020), arXiv:1908.01518.
- [25] CMS, A. M. Sirunyan *et al.*, JHEP **07**, 115 (2020), arXiv:2004.00602.
- [26] E.-C. Aschenauer *et al.*, (2015), arXiv:1501.01220.
- [27] H. Liu, *Talk given at RIKEN BNL Workshop Jet Observables at the Electron-Ion Collider*, 2020.
- [28] D. Krohn, M. D. Schwartz, T. Lin, and W. J. Waalewijn, Phys. Rev. Lett. **110**, 212001 (2013), arXiv:1209.2421.
- [29] W. J. Waalewijn, Phys. Rev. D **86**, 094030 (2012), arXiv:1209.3019.
- [30] G. F. Sterman and S. Weinberg, Phys. Rev. Lett. **39**, 1436 (1977).
- [31] B. Jager, M. Stratmann, and W. Vogelsang, Phys. Rev. D **70**, 034010 (2004), arXiv:hep-ph/0404057.
- [32] S. D. Ellis, C. K. Vermilion, J. R. Walsh, A. Hornig, and C. Lee, JHEP **11**, 101 (2010), arXiv:1001.0014.
- [33] J. Collins *Foundations of perturbative QCD* Vol. 32 (Cambridge University Press, 2013).
- [34] X. Liu and F. Petriello, Phys. Rev. D **87**, 014018 (2013), arXiv:1210.1906.
- [35] P. Sun, B. Yan, C.-P. Yuan, and F. Yuan, Phys. Rev. D **100**, 054032 (2019), arXiv:1810.03804.
- [36] M. G. Buffing, Z.-B. Kang, K. Lee, and X. Liu, (2018), arXiv:1812.07549.
- [37] Z.-B. Kang, K. Lee, J. Terry, and H. Xing, Phys. Lett. B **798**, 134978 (2019), arXiv:1906.07187.
- [38] Y.-T. Chien, D. Y. Shao, and B. Wu, JHEP **11**, 025 (2019), arXiv:1905.01335.
- [39] X. Liu, S.-O. Moch, and F. Ringer, Phys. Rev. Lett. **119**, 212001 (2017), arXiv:1708.04641.
- [40] T. Sjostrand, S. Mrenna, and P. Z. Skands, Comput. Phys. Commun. **178**, 852 (2008), arXiv:0710.3820.
- [41] D. W. Sivers, Phys. Rev. D **41**, 83 (1990).
- [42] A. Bacchetta *et al.*, JHEP **02**, 093 (2007), arXiv:hep-ph/0611265.
- [43] M. Cacciari, G. P. Salam, and G. Soyez, Eur. Phys. J. C **72**, 1896 (2012), arXiv:1111.6097.
- [44] T. Becher, M. Neubert, L. Rothen, and D. Y. Shao, Phys. Rev. Lett. **116**, 192001 (2016), arXiv:1508.06645.
- [45] M. G. Echevarria, A. Idilbi, Z.-B. Kang, and I. Vitev, Phys. Rev. D **89**, 074013 (2014), arXiv:1401.5078.
- [46] A. Bacchetta, F. Delcarro, C. Pisano, and M. Radici, (2020), arXiv:2004.14278.
- [47] HERMES, A. Airapetian *et al.*, (2020), arXiv:2007.07755.